RADC-TR-86-137
Final Technical Report
September 1986

STUDIES OF ELECTRICAL ACTIVATION AND IMPURITY MIGRATION IN ION IMPLANTED INDIUM PHOSPHIDE

AD-A174 723

The University of Texas at Austin

Ben G. Streetman

APPROVED FOR PUBLIC RELEASE; DISTRIBUTION UNLIMITED

DTIC
ELECTE
DEC 03 1986
S   D
D

DTIC FILE COPY

ROME AIR DEVELOPMENT CENTER
Air Force Systems Command
Griffiss Air Force Base, NY 13441-5700

86 12 03 043

This report has been reviewed by the RADC Public Affairs Office (PA) and is releasable to the National Technical Information Service (NTIS). At NTIS it will be releasable to the general public, including foreign nations.

RADC-TR-86-137 has been reviewed and is approved for publication.

APPROVED: D. EIRUG DAVIS
Project Engineer

APPROVED: HAROLD ROTH, Director
Solid State Sciences Division

FOR THE COMMANDER: JOHN A. RITZ
Plans and Programs Division

AD-A174713

REPORT DOCUMENTATION PAGE

1a REPORT SECURITY CLASSIFICATION	1b. RESTRICTIVE MARKINGS
UNCLASSIFIED	N/A

2a. SECURITY CLASSIFICATION AUTHORITY	3. DISTRIBUTION / AVAILABILITY OF REPORT
N/A	Approved for public release; distribution unlimited
2b. DECLASSIFICATION / DOWNGRADING SCHEDULE	
N/A	

4. PERFORMING ORGANIZATION REPORT NUMBER(S)	5. MONITORING ORGANIZATION REPORT NUMBER(S)
N/A	RADC-TR-86-137

6a. NAME OF PERFORMING ORGANIZATION	6b OFFICE SYMBOL (If applicable)	7a. NAME OF MONITORING ORGANIZATION
University of Texas at Austin		Rome Air Development Center (ESM)

6c. ADDRESS (City, State, and ZIP Code)	7b ADDRESS (City, State, and ZIP Code)
Office of Sponsored Projects Austin TX 78712	Hanscom AFB MA 01731-5000

8a. NAME OF FUNDING / SPONSORING ORGANIZATION	8b OFFICE SYMBOL (If applicable)	9 PROCUREMENT INSTRUMENT IDENTIFICATION NUMBER
Rome Air Development Center	ESM	F19628-84-K-0030

8c. ADDRESS (City, State, and ZIP Code)	10. SOURCE OF FUNDING NUMBERS			
	PROGRAM ELEMENT NO.	PROJECT NO.	TASK NO.	WORK UNIT ACCESSION NO.
Hanscom AFB MA 01731-5000	61101F	LDPF	16	C4

11 TITLE (Include Security Classification)

STUDIES OF ELECTRICAL ACTIVATION AND IMPURITY MIGRATION IN ION IMPLANTED INDIUM PHOSPHIDE

12 PERSONAL AUTHOR(S)
Ben G. Streetman

13a. TYPE OF REPORT	13b. TIME COVERED	14. DATE OF REPORT (Year, Month, Day)	15 PAGE COUNT
Final	FROM ____ TO ____	September 1986	60

16. SUPPLEMENTARY NOTATION

This effort was funded totally by the Laboratory Directors' Fund

17	COSATI CODES		18 SUBJECT TERMS (Continue on reverse if necessary and identify by block number)
FIELD	GROUP	SUB-GROUP	Indium phosphide,
20	02		semi-insulation
			rapid annealing

19. ABSTRACT (Continue on reverse if necessary and identify by block number)

Studies have been conducted on semi-insulation stability and implant activation during both furnace and rapid thermal annealing. Various encapsulants have been used and phosphorus has been co-implanted to overcome unequal recoil of the indium and phosphorus. The surface morphology is maintained after furnace annealing to 750^6 by both phosphorus silicon glass and silicon nitride and photoluminescence indicates few As or Fa vacancies. Rapid thermal annealing suppresses phosphorus vacancy formation and prevents the occurrence of any n-type surface conductivity.

20. DISTRIBUTION / AVAILABILITY OF ABSTRACT	21 ABSTRACT SECURITY CLASSIFICATION
☐ UNCLASSIFIED/UNLIMITED ☒ SAME AS RPT ☐ DTIC USERS	UNCLASSIFIED

22a NAME OF RESPONSIBLE INDIVIDUAL	22b TELEPHONE (Include Area Code)	22c OFFICE SYMBOL
Dr. D. Eirug Davies	(617) 337-3921	RADC (ESME)

DD FORM 1473, 84 MAR   83 APR edition may be used until exhausted
All other editions are obsolete

SECURITY CLASSIFICATION OF THIS PAGE

PUBLICATIONS FROM THIS WORK

Conference Presentations

B. G. Streetman and C. W. Farley, "Simulation of Concentration-Dependent Diffusion During the Annealing of Ion-Implanted Compound Semiconductors," Electrochemical Society Symposium on Compound Semiconductors (New Orleans, Oct. 7-12, 1984). Abstract published in Journal of the Electrochemical Society 131, 468C (Nov. 1984).

B. G. Streetman, The Electrochemical Society (Toronto, May 1985), "Ion Implantation in Compound Semiconductors."

T. R. Block, C. W. Farley, and B. G. Streetman, "Temperature Response of GaAs and InP in a Rapid Thermal Annealing System." SPIE (Los Angeles, January 1986).

Thesis Publications

Mezenner, Rabah, "Encapsulation and Annealing of Gallium Arsenide and Indium Phosphide." MS, 1984.

C. W. Farley, "Implantation and Annealing of Ion Implanted Compound Semiconductors." MS, 1984.

Journal Articles (in preparation)

C. W. Farley, T. S. Kim, and B. G. Streetman, "Encapsulation and Annealing Studies of Semi-Insulating InP."

C. W. Farley and B. G. Streetman, "Simulation of Anomalous Diffusion of Acceptors in Compound Semiconductors."

C. W. Farley, T. R. Block, B. G. Streetman, and M. Anthony, "Suppression of Si Diffusion into Semi-Insulating Fe-Doped InP Using Rapid Thermal Annealing."
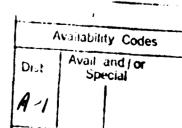
QUALITY INSPECTED 1

Availability Codes

Dist	Avail and / or Special
A-1	

i

TABLE OF CONTENTS

Page

AFOSR/RADC Final Progress Report: Overview

Over the past year, we have performed a number of experiments addressing the implantation and annealing of SI InP:Fe. Annealing studies include the effects of anneal time (where the time varies from several seconds for a rapid thermal anneal to sixty minutes for conventional furnace anneals), anneal temperature ($550^{\circ}C$ to $750^{\circ}C$), various encapsulants (doped and undoped oxides and nitrides), and varying P content in PSG caps. The annealing behavior of samples from different vendors were also studied. Implantation studies have focused on the effect of unequal recoil of In and P during implantation, the implications of this phenomenon on the activation of amphoteric dopants, and the ability of dual implants to correct for this effect. In the dual implant study, both the energy and the type of the dual implant were varied.

We have solved the basic problems of encapsulation needed for annealing (both furnace and transient). Both SiN and PSG caps show good surface morphology for furnace anneals up to $750^{\circ}C$ and transient anneals up to $925^{\circ}C$. Preliminary photoluminescence measurements on furnace annealed GaAs show few As or Ga vacancies for anneals up to $900^{\circ}C$. InP shows similar behavior to about $750^{\circ}C$.

We have also developed a diffusion simulation package which has allowed us to investigate models of the diffusion of acceptors in GaAs and InP. This simulation method has a wide range of applications, including use in modeling the diffusion coefficient of Be in InP:Fe as well as more general cases in which through the use of the Boltzmann-Matano transform (modified for implants), we can find the diffusion coefficient as a function of impurity concentration from which we can predict annealing behavior for different anneal conditions.

Results of the annealing studies showed some very interesting trends. Furnace anneals have been evaluated using PL and Hall measurements. PL emission from the BA/DA band is interpreted as resulting from both Fe depletion from the near surface region and indiffusion of Si donors from the cap. We find that the BA/DA intensity

grows with anneal time and temperature, and this increase is less dramatic for PSG and PSG/Si_3N_4 caps than for Si_3N_4 or SiO_2 caps, or for anneal in a phosphine overpressure. Hall measurements confirm this interpretation: an n-type conducting layer is formed upon annealing, except in the case of phosphine overpressure anneals. The role of Fe depletion in the increase in the BA/DA is confirmed by capped anneals of undoped InP, which shows almost no increase in the BA/DA emission. Rapid thermal annealing has been successful in suppressing the formation of a surface conducting layer; however, a broad deep level emission is seen for substrates from some vendors. This emission has been attributed to other transition metals (Mn, Cu, and Cr) which also presumably getter to the surface during annealing. It is believed that these elements are present as contaminants of the Fe used in crystal growth, which emphasizes the need for extremely pure starting materials.

Considerable variation in annealing behavior was seen for material prepared by different techniques as well as for material supplied by different vendors. In particular, LEC material from Sumitomo showed a number of unexplained transitions which appeared upon annealing. The nature of these transitions is being further investigated, but it is known that these are not related to the encapsulant, since they appeared for the anneals in a PH_3 overpressure. Also, the LPE material showed behavior different from the LEC substrates, with another peak very close to the DA line attributed to a Si donor. This line has been tentatively attributed to a transition involving a Si acceptor, since one would expect the probability of Si residing on a P site would be greater for the material grown in an In melt. In general, most of the substrates examined showed an increase in integrated PL intensity upon annealing, which suggests that there is damage in the crystal remaining from the lapping and polishing process.

Rapid thermal anneals also show drastically different PL spectra and suggest that the formation of P vacancies is suppressed by the short anneal time. The general shape of the PL spectra changes little as the anneal time increases from three to ten seconds, with the exception that the intensity of the broad deep level emission is reduced dramatically. The emission we have attributed to the P vacancy appears more strongly in

2

phosphine overpressure anneals (the phosphine overpressure is much less than the partial pressure of P over InP) and studies using varying P content in PSG layers and varying phosphine overpressure are in progress to confirm this assignment. The variation in the annealing behavior of substrates from one vendor to another is quite large, and a number of transition metals are seen in some substrates (e.g. those from Sumitomo Electric). This variation emphasizes the need to characterize substrates before use, and underlines the importance of the purity of starting materials.

The dual implant studies have also produced some very interesting results. We have varied the energy of a P co- implant, and both PL and Hall measurements confirm predictions made on the basis of the theory of unequal recoil. Shallow P implants where the peak of the P implant is on the surface side of the Si implant show more enhancement in activation than do deep P implants, although both produce greater activation efficiency than for the Si implant alone. We have also investigated N co-implants and using PL have found evidence of a deep level tentatively assigned to a (Si,N) complex. This conclusion is supported by Hall measurements which show reduced activation efficiency as a result of the N co-implant. More extensive studies are in progress to clarify this point.

Chapter 1. Simulation of Anomalous Acceptor Diffusion in Compound Semiconductors

1.1 Introduction

Impurity migration presents significant impediments to the development of diffusion and implantation technologies for compound semiconductor devices. Impurity migration during device processing is controlled not only by the properties of the impurity and the host material but also by defects produced during crystal growth and subsequent processing steps. The role of implantation-induced defects in impurity migration during annealing has been reviewed (1). Such migration is often complicated by unusual impurity diffusion behavior in undamaged regions of the crystal. A particular problem is fast interstitial-substitutional diffusion, which makes it difficult to retain the shape of the implanted profile or to predict diffusion using conventional theory. This type of diffusion usually produces shoulders or tails in the post-anneal impurity profiles and appears to be dominant for acceptor impurities such as Zn, Be, Cd, Mn, Fe, and Mg, but not for donors such as Si, Sn, and Se. This suggests that the ionic charge state of the impurity may strongly influence the diffusion mechanism. Interstitial-substitutional mechanisms have been proposed for Zn in GaAs (2) and InP (3), Cd in GaAs (4) and InP (5), Mn in InP (6), and Fe (7) and Cr (8) in GaAs. The similarity between the annealing behavior of these impurities and that of Be and Mg in InP suggests that Be and Mg diffuse through this mechanism in InP.

Fast interstitial-substitutional diffusion of acceptors is strongly concentration-dependent and is very sensitive to the concentration of vacancies on the column III sublattice. An impurity which is diffusing in this mode will hop from one interstitial site to another until it comes to rest on a substitutional site which was previously vacant. Therefore, the substitutional fraction of a given impurity will increase as the supply of vacancies increases and decrease as that supply decreases. Thus, the supply of vacancies

4

will strongly influence the diffusion of impurities which migrate at different rates in substitutional and interstitial modes. In compound semiconductors, substitutional diffusion is much slower than interstitial diffusion so that vacancy depletion produces enhanced diffusion. An example of the importance of vacancy supply is the fact that diffusion of Zn and Cd in GaAs (9) and Zn in GaAsP (10) can be modified by co-implanting As or P. Such co-implantation reduces Zn and Cd diffusion by increasing the substitutional fraction of these impurities on column III sites and thereby inhibiting fast interstitial diffusion. However, the anomalies observed for most acceptors cannot be explained entirely by changes in vacancy supply. Since there should be a depletion of vacancies as the indiffusing impurity occupies vacant lattice sites, one would expect diffusion to be fastest at the highest impurity concentrations. However, the fastest diffusion actually occurs at impurity concentrations which are several orders of magnitude lower than the maximum concentration present in the sample (2-4,6,13-18). In fact, this fast diffusion appears to be governed by the level of background impurities in the substrate (13-18).

The diffusion of acceptors in doped semi-insulating (SI) or n-type material is complicated by a change in the activity coefficient ($a=p/N_A$) and by the electric field produced at the diffusion front. In SI material, the compensating impurity pins the Fermi level near mid-gap; therefore, the activity coefficient of shallow acceptors rapidly increases as the concentration of these acceptors exceeds that of the deep acceptors and free holes are created. Furthermore, an electric field is created at the p-i junction, retarding the diffusion of acceptors which are positively charged during interstitial diffusion (11). Also, the electric field at p^+-i junctions extends into the p^+ region due to the gradient in the hole concentration produced by the implanted or diffused distribution. These same effects occur for diffusion into n-type material when the acceptor concentration exceeds the donor concentration.

Because concentration-dependent diffusion is seen for most impurities in compounds, diffusion models should take this concentration dependence into account in order to be useful. Simulations based on the assumption that the diffusion coefficient is a constant yield results which are accurate only in a portion of the impurity profile. More accurate simulation results have been obtained by dividing the profile into several regions, within which the diffusion coefficient is assumed to be constant (12). Profiles calculated in this way agree

5

quite well with the secondary ion mass spectroscopy (SIMS) profiles from which model parameters were derived, but this approach offers little insight into the nature of the diffusion mechanism involved.

This chapter describes our efforts to understand anomalous redistribution in compound semiconductors by testing models of the diffusion coefficient which include the effects of temperature, impurity concentration, and outdiffusion. First, the anomalous diffusion which motivated this effort is reviewed. Second, a correct expression for the diffusion equation for a concentration-dependent diffuson coefficient is presented. Third, the diffusion models used to simulate the anomalies are explained and successful simulations of the behavior of Be in InP are discussed. Fourth, explanations of the anomalous Be diffusion and the depletion of Fe and Cr seen for Be implants into SI InP are offered. Finally, the general implications of fast interstitial-substitutional diffusion of acceptor and compensating impurities for doping by ion implantation are discussed.

1.2 Background

This research focuses on simulating the role of impurity concentration and outdiffusion in the anomalous diffusion of implanted Be and Mg during thermal annealing, reported by Oberstar et al. (13, 14) and Vaidyanathan et al. (15). These experimental results contain several interesting features which are common to the behavior of both Be and Mg, and from this point forward we will consider only Be. First, SIMS profiles of annealed Be implants into InP (Fig. 1) show that for high implant doses Be penetrates deeply, forming long flat diffusion tails into the bulk, with a steep diffusion front. Second, anomalous deep diffusion was reported for implants into SI InP substrates, but not for samples grown by vapor phase epitaxy (VPE). Other workers have observed that for acceptor diffusion or implantation into n-type material, deep penetration of the acceptor occurs when the acceptor concentration is only slightly greater than the donor concentration (6,16-18). Anomalous migration has been seen for Mn implanted into InP (6) and for Zn implanted or diffused into GaAs(17) and InP(18) crystals with very low carrier concentrations. In particular, a deeply penetrating front is observed at acceptor levels corresponding to the donor concentration in the virgin substrates. Third, this front penetrates less as the anneal temperature increases, contrary to expectations based on conventional diffusion theory. Fourth, at all anneal temperatures, the deeply penetrating front moves little between 15 and 30 minutes, suggesting that the deep penetration occurs in the first few minutes of the anneal (Fig. 1). This finding is supported by recent work on short time annealing of Mg implants into InP which shows that the front penetrates to a depth of 2 microns after only six minutes at $800^{\circ}C$ (16). Finally, in this region of enhanced Be diffusion, the Fe is displaced and only about 10% of the original Fe concentration remains in the region of the flat tail. At the front, where the Be concentration drops below the SIMS detection limit, the Fe concentration returns to its original level.

1.3 Diffusion Simulation Method

Diffusion simulation is accomplished with a modified form of the diffusion equation. In cases where the diffusion coefficient is not constant, the diffusive flux cannot be expressed as the product of a diffusion coefficient and a concentration gradient, but must instead be expressed as the product of a concentration-mobility product and a chemical potential gradient. These phenomenological equations take the form

$$J_I = -\sum_i L_{iI}(\partial U_I/\partial C_i)(\partial C_i/\partial x) \qquad [1]$$

$$= -\sum_i D_{iI}(\partial C_i/\partial x) \qquad [2]$$

where L_{iI} is the phenomenological coefficient linking the flux of the interstitial species (J_I) with a gradient in the concentration of the ith species (C_i) and the chemical potential of the interstitial species (U_I). D_{iI} is the diffusion coefficient for the interstitial species due to a gradient in the concentration of the ith species. In a substitutional-interstitial system where the substitutional species are considered not to move, the above summations reduce to

$$J_I = -L_{II}(\partial U_I/\partial C_I)(\partial C_I/\partial x) = -D_{II}(\partial C_I/\partial x) \qquad [3]$$

so that

$$D_{II} = L_{II}(\partial U_I/\partial C_I) \qquad [4]$$

Although the substitutional species do not migrate, they do affect the diffusion of the interstitial species since $\partial U_I/\partial C_I = (\partial U_I/\partial C_S)(\partial C_S/\partial C_I)$ where C_S is the concentration of the substitutional species. In compensated semiconductors, one must consider that the number

8

of free carriers is not necessarily linearly related to the concentration of substitutional impurities. This non-linearity affects the chemical potential gradient and thus the diffusion coefficient and is expressed through a departure of the activity coefficient from a value of 1. For the case of no applied fields and a gradient in both the activity coefficient and the concentration of the substitutional species,

$$D_{II} = L_{II} [1 + (C_S/a)(\partial a/\partial C_S)(\partial C_S/\partial C_I)] \qquad [5]$$

Then, when we write the diffusion equation using the diffusion coefficient given in [5], we find

$$(\partial C_I/\partial t) = \{D_{II} + (\partial D_{II}/\partial C_I)\} (\partial^2 C_I/\partial x^2) \qquad [6]$$

where the term $\partial D_{II}/\partial C_I = (C_S/a)(\partial a/\partial C_S)(\partial^2 C_S/\partial C_I^2)$. Thus an effective diffusion coefficient $D_{II}' = D_{II} + (\partial D_{II}/\partial C_I)$ can be used in the diffusion equation, and the original diffusion coefficient can be recovered given that $\partial^2 D_{II}/\partial C_I^2 << D_{II}$. Thus, we have simplified the problem to a conventional diffusion simulation where the diffusion coefficient is determined for each simulation grid point. If we take the diffusion equation to discrete form and expand the derivatives using Taylor series expansions (19), C(x,t) becomes $C_{i,j}$, the concentration in the ith depth interval and the jth time interval where the depth increment h is defined by x = ih, and the time step k is defined by t = jk. Then,

$$C_{i,j+1} = C_{i,j} \times (1 - 2 \times q_i) + C_{i+1,j} \times (q_i + dq/4)$$

$$+ C_{i-1,j} \times (q_i - dq/4) \qquad [7]$$

where the normalized diffusion coefficient is

9

$$q_i = 2 \times h/k^2 \times D_{i,j} \qquad\qquad [8]$$

and its gradient is

$$dq = q_{i+1} - q_{i-1} \qquad\qquad [9]$$

The time step k was chosen to allow the largest possible fraction q of the impurities to diffuse during a simulation time step. From the results of simulations which considered values of q from 0.1 to 0.99 it was determined that a value of q equal to 0.9 could be used without introducing numerical instabilities. Given q_{max}, the value of k can be determined from

$$k = h^2 / (q_{max} \times D_{max}) \qquad\qquad [10]$$

since D_{max}, the largest possible value of the diffusion coefficient can be calculated in a given simulation.

1.4 Results for Be in SI InP.

In our simulations of the results of Oberstar et al. (13,14), the unannealed impurity profile is assumed to be a Gaussian resulting from a 10^{15} cm^{-2} implant, with a projected range of 4800Å and a straggle of 800Å. A model has been proposed to describe the experimental results for Be migration during annealing which involves reduced diffusion at higher concentrations (20). This reduction model has since been modified to include a reduction at low concentrations which produces a slightly steeper diffusion front more closely resembling the experimental data of Oberstar et al. (13). A reduction in the diffusion coefficient at high concentrations is necessary to produce the concave section of the profile observed by Oberstar whereas a reduction at low concentrations is necessary to produce the steep diffusion front. The shape of the profile is found to be largely dependent on the degree to which the diffusion coefficient is reduced at high concentrations. For a small reduction, the profile shows a small shoulder at C_{max} whereas for a large reduction the shoulder extends into the bulk, forming a deeply penetrating tail similar to those reported by Oberstar. When the diffusion coefficient is large, the depth of the front is critically dependent on the reduction factor. Simulations using this model show retrograde behavior (20), but in one respect fail to reproduce accurately Oberstar's results. As the anneal temperature increases, simulated profiles become more peaked, whereas experimental profiles diffuse and flatten out. Also, the activation energies needed to fit the experimental data cannot be attributed to any physical processes. This demonstrates that the model is inappropriate to the phenomenon being simulated, and suggests that the problem should be treated in terms of enhanced diffusion within a limited range of impurity concentrations.

An enhancement model for the diffusion coefficient has been developed which is very similar to the previously discussed reduction model. In the enhancement model, we have

$$D_{enh}(C,T) = \begin{cases} D_o(T), & C < C_{min} \, , \, C > C_{max} \\ \\ D_o(T) \times D_e(T), & C_{min} < C < C_{max} \end{cases} \qquad [13]$$

11

where $\qquad D_o(T) = D_o \times \exp(-U_o/kT)$

and $\qquad D_e(T) = D_e \times \exp(U_e/kT)$

In the enhancement model, the diffusion behavior is changed in the region where $C_{min} < C < C_{max}$, unlike in the reduction model, where the diffusion coefficient is changed in regions where $C < C_{min}$ or $C > C_{max}$. The enhancement model emphasizes the importance of enhanced diffusion in a limited range of impurity concentrations. It also deemphasizes the importance of reduced diffusion due to gettering at the peak of the implant in explaining the deep penetration and the flat tail of the diffusion profile. As with the reduction model, we must have $U_o < U_e$ in order to observe reduced penetration of the diffusion front at higher temperatures. The fact that D_e varies as $\exp(U_e/kT)$ and not $\exp(-U_e/kT)$ implies that diffusion is retarded by the enhanced thermal generation of vacancies which occurs at higher temperatures. *Such a dependence implies that Be is diffusing by an interstitial-substitutional mechanism.* With this model, reduced penetration and spreading of the peak of the profile are accurately simulated (Fig. 2). However, the amount of impurity remaining at the peak is much more than is observed experimentally; we attribute this to outdiffusion during annealing, which is not taken into account and which Oberstar et al. report to be severe at higher temperatures (13).

Outdiffusion is treated by allowing it to dominate over some depth from the surface (or the encapsulant/semiconductor interface), x_o. Then,

$$D(x,C,T) = \begin{cases} D_{out}(T), & x < x_o \\ D_{enh}(C,T), & x > x_o \end{cases} \qquad [14]$$

12

where $\quad D_{out}(T) = D_{out} \times \exp(-U_{out}/kT)$

and $\quad U_{out} = 1.0$ eV

In order to determine the role of outdiffusion in producing the profiles shown in Fig. 1, the depth (x_O) and magnitude (D_{out}) of outdiffusion are varied. The influence of varying the depth is shown in Fig. 3. It can be seen that the depth to which outdiffusion dominates (x_O) does not affect the behavior of the deeply penetrating front unless x_O exceeds the depth at which the pre-anneal impurity concentration is less than C_{max}. That is, outdiffusion affects only the surface region of the profile unless x_O reaches the region of enhanced diffusion. Using a value of 6000 Å for the depth of outdiffusion, we investigate the effect of varying the magnitude of the diffusion coefficient. The results of these simulations are shown in Fig. 4. Here it is clear that the peak impurity concentration can be changed over several orders of magnitude through outdiffusion without substantially changing the bulk (enhanced) diffusion behavior. This justifies developing explanations of the diffusion behavior in the surface and bulk regions separately.

We use the Boltzmann-Matano transform (21) to verify the accuracy with which the simulations implement the specified diffusion coefficients and to determine the effect of outdiffusion of the diffusion coefficient. This transform allows one to determine the diffusion coefficient as a function of concentration from either an experimental or a calculated profile of impurity concentration versus depth. By evaluating the flux past a plane in which the concentration $C(x) = C_O$, and evaluating the concentration gradient at that point, one can extract the diffusion coefficient at that concentration, $D(C_O)$. This transform has been developed (21) for surface diffusions so that for implants the depth has to be measured relative to the projected range (to first order) or relative to that depth at which that same concentration existed at t=0 (to second order). This transform will be least accurate at the

13

lowest and highest concentrations since the slope is most difficult to determine in these regions. In our analyses, the transform seems to become inaccurate only at high concentrations when the slope of the impurity profile becomes very small. All plots of diffusion coefficient versus impurity concentration for calculated profiles show curvature at high concentrations which is the result of this numerical error. However, this anomaly did not affect our ability to interpret the results of the transform since the anomaly occurred at much higher concentrations than those in which we were interested. Using this transform on calculated profiles we find that accurate simulations can be carried out for k<0.9, and that the effects of outdiffusion on the diffusion coefficient in the bulk are negligible for $x_0 < 6000$ Å.

We also analyzed the experimental profiles using this transform and compared the diffusion coefficient obtained from these profiles with that obtained from calculated profiles. We find agreement between the simulated and experimental diffusion coefficients within a factor of 5. It is clear from this comparison that the B-M transform could be used on experimental data to generate the diffusioncoefficient parameters needed for the model. All features of the experimentally measured profiles can be simulated accurately and next a physical description of the diffusion process is discussed.

1.5   Discussion

Results of the simulations presented in the previous section show that most features of the anomalous diffusion observed for Be in SI InP are explained by an enhancement of the diffusion coefficient in a narrow range of impurity concentrations. The temperature dependence of the enhancement necessary to simulate the experimental profiles shows that Be diffusion occurs through an interstitial-substitutional mechanism. The simulations do not specify the mechanisms which give rise to this enhancement, but we can speculate on several plausible mechanisms based on what is known about acceptor behavior in compound semiconductors.

Based on our simulations we can make a general statement about the experimentally observed Be migration. Release of Be atoms from the high concentration regions appears to

14

be the rate-limiting factor in the diffusion process, but the rate of release cannot be described simply. It may be that relatively immobile damage clusters created by high dose implants are not annealed out at lower temperatures and their limited gettering ability allows the rapid diffusion seen for low anneal temperatures. When annealed at higher temperatures, these clusters dissociate into rapidly diffusing point defects whose greater gettering ability slows the diffusion of Be. This hypothesis is consistent with the dose dependence observed for the anomalous diffusion since clustering should be more pronounced for higher implant doses and this is where reduced penetration at higher temperatures is observed. This explanation also fits the time dependence observed: as the anneal proceeds, diffusion at low concentrations becomes less significant and the profile increasingly resembles the result of Fickian diffusion. Presumably this results because damage clusters are annealed out early in the anneal cycle and further annealing merely allows diffusion which is controlled by thermally generated vacancies to occur. However, the fact that simulations of the effect of outdiffusion show that changing diffusion behavior near the surface has little effect on bulk diffusion behavior, we feel that these factors can only explain diffusion behavior in the near-surface region and may not be as important as outdiffusion of the impurity from the semiconductor surface.

At least two other phenomena which may enhance Be migration should become much stronger in the same concentration range and are the most probable causes of the anomalous bulk diffusion behavior observed; gradients in the activity coefficient and electric fields produced at the p-i or p-n junction formed at the diffusion front. Consider first the effect of changes in the activity coefficient. When Be_{In} is less than Fe_{In}, the activity coefficient is zero since the addition of Be atoms on In sites does not produce free holes. When Be_{In} exceeds Fe_{In}, the activity coefficient of Be rises abruptly: the Fermi level becomes unpinned when the deep acceptor levels are insignificant compared to the shallow acceptor levels due to substitutional Be. For acceptor diffusion in n-type material this change in the activity coefficient occurs when Be_{In} exceeds the donor concentration. In either case, $\partial a/\partial C_S$ and therefore the diffusion coefficient become dramatically larger when the acceptor concentration exceeds that of the deep compensating impurity or the shallow donor. At high Be

15

concentrations the available In sites become saturated so that no more Be atoms can be located on In sites. In this case, $\partial C_S/\partial C_I$ goes to zero, and the diffusion coefficient returns to its value for low Be concentrations. We believe that anomalous diffusion was not detected by Oberstar et al. (13) for implants into VPE material because these substrates were n-type with carrier concentrations of about 10^{14} cm^{-3}. In fact, anomalous diffusion may have occured, but it would have appeared at 10^{14} Be cm^{-3}, which is an order of magnitude below the SIMS detection limit.

Be migration is also affected by the electric fields produced by the carrier concentration gradients formed during annealing. When Be_{In} exceeds Fe_{In}, there is net space charge from Be acceptors and an electric field is produced at the p-i junction formed by the diffusing Be which retards the diffusion of positively charged interstitial Be atoms for Be_{In} greater than Fe_{In}. An additional component of the electric field is developed in the p$^+$ region due to the gradient in the hole concentration resulting from the implant profile which also retards the diffusion of interstitial Be$^+$. These effects are much more difficult to quantify since little is known about the hole concentration profile during annealing.

Be indiffusion is associated with substantial depletion of Fe and Cr, and the compensating impurity levels return to pre-anneal values where the Be concentration drops off to the SIMS detection limits. The minimum Fe concentrations are $\sim 10^{16}$ cm^{-3}, but Cr depletes down to $\sim 10^{15}$cm^{-3}. These values correspond roughly to the solid solubilities of Fe and Cr in InP at the anneal temperatures, which suggests that solubility is an important factor in the depletion. During crystal growth, compensating impurities are incorporated into the lattice in concentrations appropriate to the solid solubility at the growth temperature, but the solubility of these impurities at the anneal temperatures is much less. Depletion of Fe and Cr may be simply a return of Fe and Cr concentrations to equilibrium levels which is assisted by Be diffusion or doping. The displacement of Fe and Cr by Be may merely reflect that the solid solubility of Be is greater than Fe or Cr at the anneal temperatures studied. A more likely explanation for the experimentally observed Fe migration is the effect of Be on the chemical potential. As Be_{In} exceeds Fe_{In}, the material becomes p-type and the potential of

16

Fe_{In} becomes higher than the Fermi level, which is moving toward the valence band. Thus, the Fe migration to regions in which Be is not present would be favored since it represents diffusion down a potential gradient. It is also probable that the energy needed for Fe to become interstitial is less in p-type than in n-type material. This hypothesis is supported by radiotracer studies of GaAs diffused with Fe (7). Fe acts as an acceptor in n-type material by the reaction

$$Fe_{Ga}^{3+} + e \longleftrightarrow Fe_{Ga}^{2+} \qquad [15]$$

whereas in p-type material the Fermi level is below the Fe_{Ga}^{2+} energy level so that Fe is seen only as Fe_{Ga}^{3+}. In this case, the Fe atom does not have to change charge state in order to become Fe_i^{3+}, so that interstitial diffusion would be enhanced in p-type material compared to n-type material and Fe would be observed to deplete from the Be-diffused region.

Anomalous diffusion through fast interstitial mechanisms appears to be widespread for acceptors in GaAs and InP. In order to reduce the amount of redistribution of these impurities during annealing, transient anneals have been employed in which the sample remains at an elevated temperature for a short period of time. Redistribution of implanted impurities has been reduced in GaAs compounds (19,22), but there are indications of a tradeoff between carrier activation and impurity redistribution (22-24). Considering the rapid nature of the deep diffusion of Be and Mg reported in InP (13-15), transient annealing appears to be one of the most promising solutions to the problem of electrical activation of implanted impurities with minimal redistribution.

17

1.6 Summary

We have developed a model which gives diffusion results similar to those observed by Oberstar for Be-implanted InP. The resulting profiles demonstrate that enhanced diffusion in a narrow band of concentrations is a critical determinant of the post-anneal impurity profile and suggest that Be may diffuse by an interstitial-substitutional mechanism in InP. Several mechanisms have been proposed to explain why Be diffusion in the bulk is slower at higher and lower Be concentrations. These include gradients in the activity coefficient, the effect of the concentration of substitutional species on the potential of the interstitial species, and electric fields formes at the p-i or p-n junction and in the p^+ regions. Outdiffusion in the near-surface region can also be included without significantly affecting the bulk diffusion behavior. It is clear that the behavior of Be implanted into SI or n-type InP can be accounted for by relatively straightforward diffusion theory and does not demand a consideration of gettering due to damage induced near the projected range of the implants. This description of the diffusion process should be applicable to a wide class of acceptors which diffuse by an interstitial-substitutional mechanism in compound semiconductors. A reasonable explanation for the depletion of Fe in the Be-diffused region has also been presented which is corroborated by results from Fe diffusion in GaAs.

A phenomenological approach to the analysis of anomalous diffusion can offer considerable insight into the processes involved. Knowledge of the concentration dependence of the diffusion coefficient may be coupled with knowledge about common diffusion mechanisms to develop explanations for observed anomalies. It is apparent from this and other work that rapid diffusion of acceptors is inherent in GaAs and InP. It appears that the development of successful transient annealing methods will be essential to the controlled activation of acceptor impurities in these compounds.

1.7 References

1. C.W. Farley and B.G. Streetman, J. Electron. Mat. **13**, 401 (1984).

2. H.C. Casey, M.B. Panish, and L.L. Chang, Phys. Rev. **162**, 162 (1967).

3. L.L. Chang and H.C. Casey, Sol. St. Elec. **7**, 481 (1964).

4. T. Itoh and Y. Kushiro, J. Appl. Phys. **42**, 5120 (1971).

5. P.K. Tien and B.I. Miller, Appl. Phys. Lett. **34**, 701 (1979).

6. R. Chaplain, M. Gauneau, H. L'Haridon, and A. Rupert, J. Appl. Phys. **58**, 1803 (1985).

7. M.R. Brozel, E.J. Fonlkes, Brian Tuck, N.K. Coosivami and J.E. Whitehouse, J. Phys. D: Appl. Phys. **16**, 1085 (1983).

8. B. Tuck and G.A. Adegboyega, J. Phys. D: Appl. Phys. **12**, 189 (1979).

9. A.A. Gavrilov, G.A. Kachurin, N.B. Pridachin and L.S. Smirnov, Sov. Phys. Semicond. **8**, 1455 (1975).

10. E.B. Stoneham and J.F. Gibbons in <u>Ion Implantation in Semiconductors,</u> (Plenum: New York), 57 (1973).

11. P. Enquist, L.M. Lunardi, G.W. Wicks, L.F. Eastman, and C. Hitzman, J. Vac. Sci. Technol. **B3**, 634 (1985).

12. J.C. Paz de Arrujo, J. Electrochem. Soc. **111**, 333 (1984).

13. J.D. Oberstar, B.G. Streetman, J.E. Baker and Peter Williams, J. Electrochem. Soc. **129**, 1312 (1982).

14. J.D. Oberstar, B.G. Streetman, J.E. Baker and Peter Williams, J. Electrochem. Soc. **129**, 1320 (1982).

15. K.V. Vaidyanathan, C.L. Anderson, H.L. Dunlap and D.E. Holmes, Nucl. Inst. and Meth. **182/183**, 631 (1981).

16. U. Konig, J. Hilgarth, and H.-H. Tiemann, J. Electron. Mater. **14**, 311 (1985).

17. G.J. van Gurp et al., J. Appl. Phys. **55**, 338 (1984).

18. M. Yamada et al., Appl. Phys. Lett. **43**, 594 (1983).

19. A.R. Mitchell and D.F. Griffiths, in "The Finite Difference Method in Partial Differential Equations," John Wiley & Sons, New York, (1980).

20. C.W. Farley and B.G. Streetman, J. Electrochem. Soc. **131**, 946 (1984).

21. J. Crank, <u>Mathematics of Diffusion</u>, Oxford University Press, London, (1956), p.232; P.G. Showmon, <u>Diffusion in Solids</u>, Mc Graw-Hill, New York, (1963), p.28.

22. S.K. Banerjee, R.Y. DeJule, K.J. Soda and B.G. Streetman, IEEE Trans. Electron Dev. **ED-30**, 1755 (1983).

23. P.M. Asbeck, D.L. Miller, E.J. Babcock and C.G. Kirkpatrick, IEEE Electron Devices Lett. **EDL-4**, 81 (1983).

24. T. Yu, K.J. Soda, and B. G. Streetman, J. Appl. Phys. $\underline{51}$, 4399 (1980).

1.8 Figure Titles

Figure 1. SIMS profiles of Be implants into InP:Fe show less penetration with increasing anneal temperature (From Ref. 13).

Figure 2. Simulation results for the enhancement model using $C_{min} = 10^{16}$ cm^{-3}, $C_{max} = 10^{17}$ cm^{-3}, $D_o = 3 \times 10^{-10}$ cm^2/s, $U_o = 0.6$ eV, $D_e = 3 \times 10^{-9}$ cm^2/s, $U_e = 1.8$ eV.

Figure 3. Simulation results showing the effect of various depths of enhanced surface diffusion using the same parameters as for Fig. 2, $D_{out} = 1 \times 10^{-6}$ cm^2/s, and $U_{out} = 1.0$ eV.

Figure 4. Simulation results showing the effect of various magnitudes of enhanced surface diffusion using the same parameters as for Fig. 2, $x_o = 6000$ Å, and $U_{out} = 1.0$ eV.
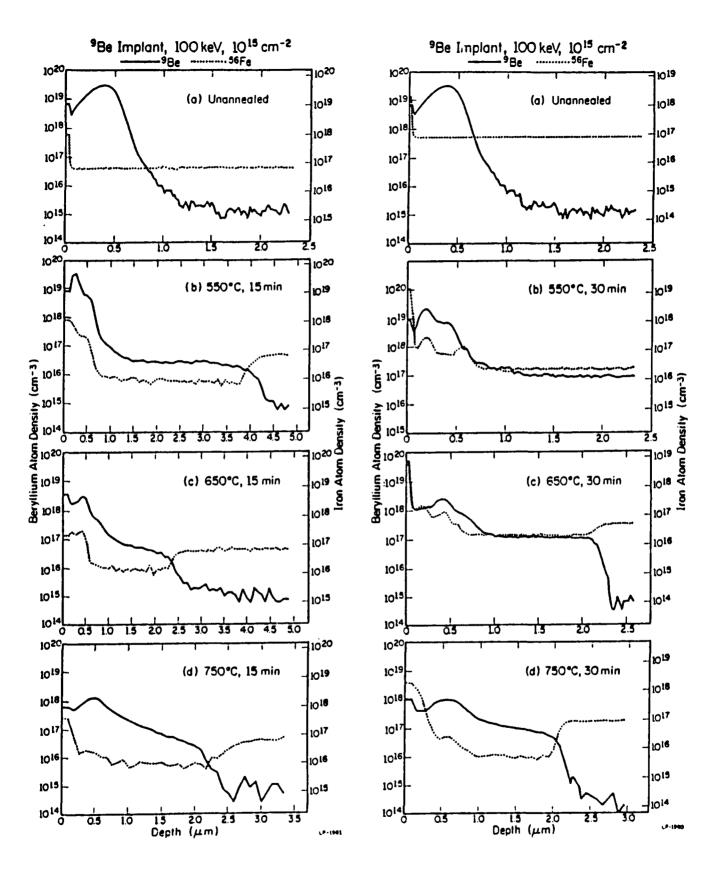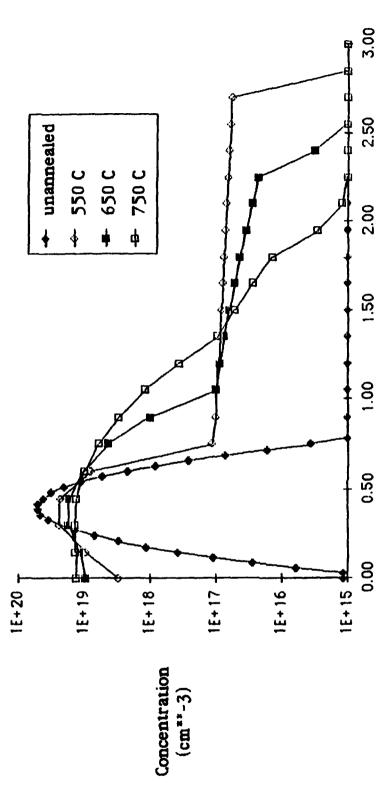
Figure 1

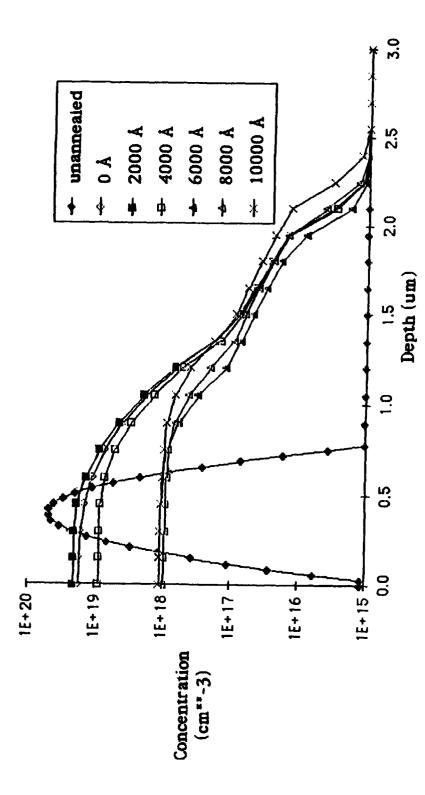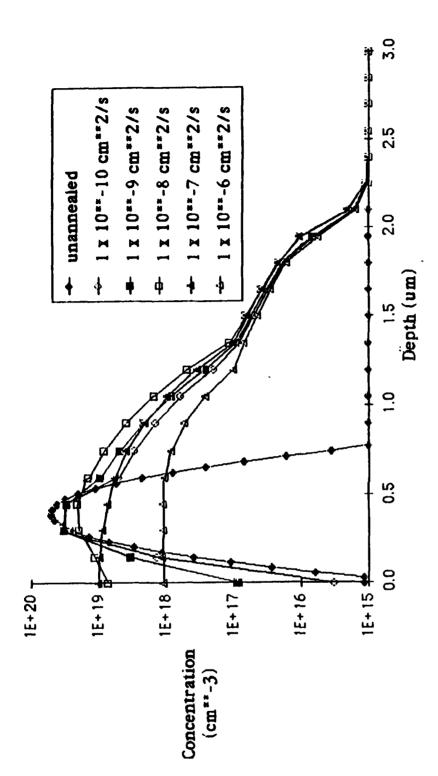Left column:

⁹Be Implant, 100 keV, 10¹⁵ cm⁻²
— ⁹Be ······ ⁵⁶Fe

(a) Unannealed

(b) 550°C, 15 min

(c) 650°C, 15 min

(d) 750°C, 15 min

Right column:

⁹Be Implant, 100 keV, 10¹⁵ cm⁻²
— ⁹Be ······ ⁵⁶Fe

(a) Unannealed

(b) 550°C, 30 min

(c) 650°C, 30 min

(d) 750°C, 30 min

Depth (μm)

Beryllium Atom Density (cm⁻³)

Iron Atom Density (cm⁻³)

Figure 2

22

Figure 3

Figure 4

24

Chapter 2. Encapsulation and Annealing Studies of Semi-Insulating InP

2.1 Introduction

Implantation into compound semiconductors such as GaAs and InP requires annealing these materials at temperatures well above that at which the column V constituent begins to preferentially evaporate [1,2]. Therefore, some means of providing an overpressure of the column V constituent must be employed. There are several reasonable methods which satisfy this requirement. An implanted GaAs sample may be annealed without a cap [3], but only for a limited time before the surface begins to dissociate. Annealing may take place in a controlled atmosphere where the overpressure is supplied by gas (typically arsine or phosphine) flowing into the annealing furnace. Although implanted GaAs is often annealed using this method, there are few reports of successful capless annealing of implanted InP [4]. This is probably due to the high vapor pressure of P over InP at typical annealing temperatures (about 100 to 1000 times that of As over GaAs). An implanted wafer may be annealed in face-to-face contact with a "dummy" wafer so that an overpressure need be maintained only in the small volume between the two wafers. Although GaAs retains good surface morphology [5], In etch pits evolve during the annealing of InP. Etch pit formation can be reduced if the "dummy" wafer is removed a small distance from the implanted wafer [6], if the InP is placed in contact with a Si_3N_4 coated wafer [5], or if the sample is held in a boat containing an InP-Sn mixture [7]. Generally the wafer must be encapsulated with a dielectric to suppress outdiffusion of host and impurity atoms at typical annealing temperatures. This study addresses some of the problems associated with annealing implanted SI InP using two promising encapsulants, silicon nitride and phosphosilicate glass.

Oberstar and Streetman have reviewed encapsulants for annealing GaAs and InP and have presented a set of properties which an ideal encapsulant for these materials should possess [8]. Three of these properties are the subject of this study. First, the deposition method and temperature should not cause incongruent evaporation of column V constituent. Second, the encapsulant

should prevent the outdiffusion of host and implanted atoms from the substrate during annealing. Third, the encapsulant should not diffuse into the substrate during the anneal. Not all of these criteria are always satisfied for commonly used encapsulants such as silicon dioxide (SiO_2), Si_3N_4, and PSG.

Another problem which is unique to the annealing of SI substrates is the redistribution during annealing of the impurity or defect responsible for the deep level compensation required to render the material semi-insulating. The migration of impurities is often dominated by interactions with implantation-induced defects, and these interactions have been reviewed recently [9]. It is well known that Cr, commonly used to form SI GaAs, getters to the encapsulant/substrate interface and depletes from a region near the surface to a depth of about one micron [10]. This anomalous migration of transition metals, and either Si indiffusion from silicon-containing caps or residual Si incorporated during crystal growth, are believed to be responsible for the formation of conducting layers on the surface of unimplanted, annealed GaAs. Similar annealing behavior has been observed for unimplanted annealed Fe-doped SI InP [11]. Since it is well known that Fe migration substantially influences the activation of low-dose implants typically used in the channel of field effect transistor (FET) structures to control threshold voltage[12], it is important to know whether this behavior is similar among substrates from different vendors, or whether there are large variations in the Fe migration behavior.

2.2   Experimental Procedures

To this end, several issues were investigated in this study. First, the formation of P vacancies and vacancy-related complexes during deposition and annealing is considered. Second, the outdiffusion of In, P, and Fe during deposition and annealing is examined and the effect of host atom outdiffusion on the indiffusion of Si from the encapsulant during annealing is studied. Finally, the redistribution of Fe during annealing is analyzed.

Various deposition parameters were used in an attempt to detect the factors responsible for the formation of P vacancies and vacancy-related complexes. In order to determine the differences between various encapsulants, SiO_2, Si_3N_4, and PSG layers were examined on substrates from the same wafer. Also, uncapped anneals in a phosphine overpressure were performed to determine the effects of the encapsulation process. For comparison of various SI substrates, crystals grown by both liquid encapsulated Czochralski (LEC) and liquid phase epitaxy (LPE) methods were examined, and SI LEC substrates from several vendors were studied.

The LEC samples used in this study were (100) SI InP doped with Fe which were obtained from Cambridge Instruments, Sumitomo Electric, CrystaComm, and AT&T Bell Labs. (100) LPE SI InP Fe-doped samples were obtained from Varian Associates. The LEC substrates were chemically-mechanically polished by the vendors with a bromine-methanol etch. After degreasing in ultrasonic rinses of TCE, acetone and methanol, residual saw and polishing damage was removed by a 1% bromine-methanol etch. The etch was quenched with methanol and the samples were rinsed with DI water and then blown dry. Encapsulant deposition or capless annealing was performed immediately after sample preparation. SiO_2 and PSG layers were deposited by the thermal decomposition of 2% silane in Ar and 2% phosphine in Ar and reaction with O_2 in a N_2 carrier gas. Oxygen-free Si_3N_4 was deposited by a plasma enhanced chemical vapor deposition (PECVD) process reported elsewhere [13]. Furnace anneals of encapsulated samples were carried out in a quartz tube furnace with flowing forming gas (~4% H_2 in N_2) at atmospheric pressure at a temperature of 750°C for 30 minutes. Capless anneals were carried out in the PECVD reactor with a phosphine partial pressure of 1 Torr, a total pressure of 50 Torr, at a temperature of 550°C for 30 minutes.

27

The effects of encapsulant deposition and annealing were characterized using differential Hall profiling measurements, PL spectroscopy, and SIMS profiling. The Hall system is similar to that reported by McLevige et al. [14], which involves the choice of sample current and magnetic field frequencies so that the resistivity and Hall voltages do not have harmonic interference from the magnetic field current. Photoluminescence measurements were carried out at 4.2K with the sample immersed in liquid He in a Janis 8DT Supervaritemp cryostat. Samples to be characterized by PL are mounted on a copper plug by embedding them in indium[15]. The sample was excited with the 5145 Å line of an Ar ion laser. The front surface PL was collected with focusing optics into the entrance slit of a one meter spectrometer. The optical output was detected using a photon counting method with an EMI 9684B (S-1 response) photomultiplier tube cooled to -100°C.

2.3 Results and Discussion

2.3.1 Encapsulation effects.

The results of PL and SIMS measurements of encapsulated unannealed samples suggests that the encapsulant deposition conditions typically used for GaAs may be undesirable for InP. SIMS profiles of as-deposited Si_3N_4 indicate that P may be lost from the surface of InP during encapsulant deposition. As can be seen in Figure 1, significant concentrations of P are seen near the surface of Si_3N_4 deposited on InP at 350°C before intentional annealing. Since the P signal decreases as we sputter through the Si_3N_4, we know that the P signal is not coming from the substrate through pinholes. The outdiffusion of P into as-deposited dielectrics on InP has not been previously reported. This may be because the levels of P are below Auger detection limits and because charging and mass interference with $^{30}SiH^+$ limits the usefulness of SIMS [11]. For these profiles, the Cameca IMS3f was operated in the high resolution mode, which allows one to distinguish between $^{30}SiH^+$ and ^{31}P. Furthermore, PL spectra of PSG encapsulated unannealed samples show that P vacancies or vacancy-related complexes may be formed when the PSG deposition temperature is greater than 300°C. We have observed a P vacancy-related emission at about 8900 Å in PL spectra of samples annealed without encapsulation in a phosphine overpressure. This emission can be identified as one related to P vacancies or vacancy-impurity complexes since it is known that the phosphine partial pressure used during these anneals (~1 Torr) is much less than the pressure of P over InP at the anneal temperature (550°C). Figure 2 shows the evolution of this emission with increasing deposition temperature for samples capped with PSG layers with a content of ~7 wt. % P as determined by energy dispersive X-ray spectroscopy. Although P vacancy formation is consistent with the appearance of P in as-deposited Si_3N_4, it is somewhat surprising that these P vacancies are formed during PSG deposition, which involves lower deposition temperatures than for Si_3N_4 layers, no possibility of plasma damage since the PSG deposition process is only thermally enhanced, and an environment of phosphine overpressure. However, Van Uitert et al. found that P evolves from the InP surface at temperatures well below 360°C, and that the vapor pressure of P over InP increases by an order of magnitude for every 45°C increase in temperature [16]. Their results are consistent with the loss of P we observe and suggest that deposition temperatures should be on the order of

29

250°C in order to suppress the loss of P from the InP surface.

2.3.2 Outdiffusion during annealing. Comparisons of PSG and Si_3N_4 capped samples suggest that Si_3N_4 is a better barrier to host atom outdiffusion than PSG. These results are consistent with findings in GaAs which showed much reduced Ga outdiffusion for Si_3N_4 capped samples than for SiO_2 or silicon oxynitride capped samples [20]. The degree to which a particular encapsulant serves as a barrier to outdiffusion of host atoms was determined from SIMS atomic profiles of ^{30}Si, ^{31}P, ^{54}Fe, and ^{113}In in the dielectric layer. As can be seen in Figure 1, only P was detected in unannealed Si_3N_4 deposited on InP at 350°C. Upon annealing, In, P, and Fe outdiffuse from the substrate into the cap and accumulate at the surface, as is shown in Figure 3. P accumulates in the upper ~1000Å of the 3000Å thick cap, but is distributed throughout the cap at concentrations several orders of magnitude lower than the surface concentration. The P concentration is everywhere about ten times greater than in the unannealed case which represents at least several monolayers of P. It is clear that Si_3N_4 does not prevent P loss from the InP surface during annealing. In outdiffusion is more severe for PSG-capped samples than for ones Si_3N_4 capped samples which is in agreement with the results of Oberstar et al. [13]. This behavior parallels the outdiffusion of Ga from GaAs through SiO_2, $Si_xO_yN_z$ and Si_3N_4 [19]. Furthermore In as a peak appears near the surface of PSG-capped samples. This accumulation either InP or In and P oxides on the surface of the film as a compound formation is not known at present whereas Fe is detected only in the top 500 Å. This profile Although the In and Fe accumulations are larger in some are found only in the upper 500-1000 Å of the film, whereas P is found throughout the encapsulant in annealed samples. Fe was detected in the upper 500 Å of a Si_3N_4 film deposited on SI InP at 350°C and annealed at 750°C for 30 minutes, although Fe was not detected in PSG capped samples similarly annealed, as is shown in Figure 4. At this point, it is not clear whether Fe does not enter the PSG or whether it enters the PSG but outdiffuses completely.

2.3.3 Si Indiffusion. We believe that the difference in Si indiffusion and doping behavior observed for PSG and Si_3N_4 capped samples can be understood in terms of In outdiffusion and Fe accumulation at the substrate surface during annealing. In outdiffusion during annealing created vacancies on the In sublattice which enhance both Si indiffusion and Si donor activity. Doping from indiffused Si is suppressed by surface accumulations of Fe, which compensates the shallow Si donor levels. The extent to which the encapsulant serves as a dopant source supplying Si donors to the substrate was determined from a comparison of SIMS atomic profiles and Hall effect carrier concentration profiles. SIMS profiling was performed on capped and annealed substrates which had their cap stripped prior to profiling to avoid sputter knock-on of Si. The surface concentration of Si is ~2 x 10^{20} cm^{-3} for all cases, but as can be seen in Figure 5, the Si concentration rapidly drops to ~1 x 10^{19} cm^{-3} at a depth less than 1000 Å. From this point, the Si concentration remains above background levels (~5 x 10^{16} cm^{-3}) to a depth of ~1.5 to 2 microns. The Si profile is almost identical for Si_3N_4 capped substrates from two different vendors, which suggests that this behavior is intrinsic to LEC SI InP. This significant indiffusion of Si suggests that Si-containing caps should not be used for furnace annealing of channel implants in InP FETs. Contrary to the results of Oberstar et al. [17], more Si indiffusion is seen for PSG capped samples than for Si_3N_4 capped ones. However, the observed result can be explained by differences in In outdiffusion behavior seen for different encapsulants. In outdiffusion creates vacancies on the In sublattice which the Si atoms can occupy, so that greater In outdiffusion produces greater Si indiffusion. This relationship between In vacancy concentration and Si indiffusion is confirmed by the reduced Si indiffusion observed for LPE SI InP substrates. Since LPE material is grown from an In-rich melt, and not in a P overpressure as is the LEC material, the concentration of In vacancies would be much smaller in the LPE substrates than in the LEC substrates, and Si indiffusion would be accordingly suppressed.

2.3.4 Comparison with GaAs. The diffusion and doping behavior of Si in InP resembles that of Si either implanted or diffused into GaAs [15,17,18] and shows a strong dependence on the cation vacancy concentration. Onuma et al. observed that the diffusion coefficient of Si implanted into GaAs is about 20 times larger when a SiO_2 cap is used than when a Si_3N_4 cap is used [18].

31

This difference is apparently due to the creation of Ga vacancies when SiO_2 is used as an encapsulant. Vaidyanathan et al. reported substantial outdiffusion of Ga through SiO_2 and silicon oxynitride layers and virtually no Ga outdiffusion through oxygen-free Si_3N_4 [20]. Onuma et al. also reported substantial indiffusion of Si from the SiO_2 cap for an unimplanted, annealed sample, which is in agreement with our findings in InP. Greiner and Gibbons [19] studied the diffusion of Si in GaAs using rapid thermal processing and found measurable conduction for samples capped with SiO_2 and annealed at 1050° C for 3 seconds whereas Si proximity annealed and Si_3N_4 capped samples showed no measurable electrical conductivity. This surface conducting layer is the result of Si indiffusion from the SiO_2 cap which was detected by SIMS profiling. Greiner and Gibbons identified the Ga vacancy concentration and the encapsulation method as important factors in Si diffusion behavior in a recent paper discussing a model for Si diffusion in GaAs [21].

2.3.5 Surface Conversion. Hall profiles were taken for samples capped with PSG and Si_3N_4, and conducting layers with a sheet electron concentration of about 2×10^{12} cm^{-2} at least 2000 Å thick were always found for annealed samples capped with PSG whereas a significant conducting layer was only occasionally found on annealed samples capped with Si_3N_4. Similar results were found by Donnelly et al. [22]. For some substrates, they observed n-type conversion of unimplanted Cr-doped GaAs capped with Si_3N_4 and annealed at 900° C for 15 minutes. The doping behavior observed for Si_3N_4 capped samples may be due to not only reduced In outdiffusion but also Fe gettering to the surface. Surface accumulations of Fe are larger and thicker for Si_3N_4-capped samples than for PSG-capped samples, and the Fe may be compensating Si donors.

The formation of these conducting layers may be completely suppressed by the use of rapid thermal annealing (RTA), in which anneal times are reduced to several seconds. For anneal schedules such as 750° C for up to 2 minutes, times which are adequate to activate high dose ($\sim 10^{15}$ cm^{-2}) implants, no surface conducting layer is detected for either PSG or Si_3N_4 capped samples [23].

2.3.6 Fe migration. The migration behavior of Fe in InP during annealing is different from that of Si, although both are known to reside predominantly on the In sublattice. As shown in Figure 6, Fe migrates to the encapsulant/substrate interface in all cases studied here. This is interpreted as gettering of Fe to damage at the interface caused by the encapsulation process, by evaporation during annealing, or by some chemical reactions between the InP and the encapsulant. Since Fe substitutes for In vacancies, one would expect that Fe diffusion and therefore surface accumulation would be enhanced by the presence of In vacancies. However, Fe accumulation does not vary directly with In outdiffusion. In fact, larger surface accumulations of Fe are seen for Si_3N_4 capped samples than for PSG capped samples. Also, extremely large accumulations of Fe are seen at the surface of the LPE substrate. Although both these results show an unexpected dependence on In vacancy concentration, they are consistent and suggest that the accumulation of Fe at the InP surface is retarded by the presence of In vacancies. These vacancies presumably result when P evaporates and an antisite defect In_P is formed, leaving a V_{In}-In_P complex.

In some cases, a region of depletion of the Fe below the original doping level is seen on the bulk side of this surface accumulation. This depletion behavior can be understood if one considers that Fe diffuses by an interstitial-substitutional mechanism, where diffusion is slowed by an increase in the supply of In vacancies. Since this effect is observed only in one of the two LEC substrates capped with Si_3N_4, it cannot be related to SI InP per se, but may be a phenomenon which is sensitive to the details of the LEC growth process used by a particular vendor. Since depletion is seen for LPE samples which are grown from an In-rich melt, this depletion may be related to a lack of In vacancies, presumably resulting from inadequate P overpressure during LEC crystal growth.

2.4 Conclusions

These studies have shown that there are many encapsulation and annealing problems unique to InP which are not encountered with GaAs. P was detected in a Si_3N_4 film deposited by PECVD at 350° C, and P vacancy-related PL transitions are observed when PSG deposition temperatures exceed 300°C. These results suggest that the deposition of dielectrics for encapsulation should take place below 300° C in order to avoid the loss of P from the surface during the encapsulation process. For the first time, P and Fe outdiffusion through dielectric encapsulants has been detected using SIMS profiling. In outdiffusion during annealing was detected as previously reported by Oberstar et al. [11], but observed Si indiffusion behavior did not confirm the results of Oberstar et al. [11]. Greater Si indiffusion observed for PSG capped samples is consistent with more significant In outdiffusion through the PSG cap than through the Si_3N_4 cap. Si indiffusion resembles the diffusion behavior of Si either implanted or diffused into GaAs, and for both InP and GaAs it is clear that the supply of vacancies on the column III sublattice is a critical determinant of Si diffusion kinetics. Surface conversion to n-type conduction after furnace anneals at 750° C for 30 minutes was observed in all cases for PSG capped samples and in some cases for Si_3N_4 capped samples, similar to behavior observed by Donnelly for Si_3N_4 capped Cr-doped GaAs. The formation of this surface layer could be suppressed by RTA for both types of encapsulants. Fe was observed to getter to the encapsulant/substrate interface and in some cases deplete from a near surface region. In contrast to the behavior of Si, accumulations of Fe were more pronounced for Si_3N_4 capped samples than for PSG capped samples. Larger surface accumulations of Fe were observed for LPE substrates compared to LEC substrates. Fe migration behavior can be understood if one considers that Fe diffuses through a substitutional-interstitial mechanism and if one assumes that In_P-V_{In} complexes are formed near the InP surface during annealing. These studies point out the need for low temperature encapsulant deposition processes and the use of RTA for controllable low dose implant activation in SI InP.

2.5 References

1. C.T. Foxon, J.A. Harvey, and B.A. Joyce, J. Phys. Chem. Solids, 34, 1693 (1973).

2. R.F.C. Farrow, J. Phys. D: Appl. Phys. 7, 2436 (1974).

3. M. Kuzuhara, H. Kohzu, and Y. Takayama, Mat. Res. Soc. Symp. Proc. 23, 651 (1984).

4. D.E. Davies, W.D. Potter, and J.P. Lorenzo, J. Electrochem. Soc. 125, 1845 (1978).

5. B. Molnar, Appl. Phys. Lett. 36, 927 (1980).

6. U. Konig, J. Hilgarth, and H.-H. Tiemann, J. Electron. Mater. 14, 311 (1985).

7. K.P. Pande, V.R.K. Nair, and O. Aina, Appl. Phys. Lett. 45, 532 (1984).

8. J.D. Oberstar and B.G. Streetman, Thin Solid Films, 103, 17 (1983).

9. C.W. Farley and B.G. Streetman, J. Electron. Mater. 13, 401 (1984).

10. M. Oshima, K. Watanabe, and S. Miyazawa, J. Electrochem. Soc. 131, 130 (1984).

11. J.D. Oberstar, B.G. Streetman, J.E. Baker, and Peter Williams, J. Electrochem. Soc. 128, 1814 (1981).

12. M. Arai, K. Nishiyama, and N. Watanabe, Jap. J. Appl. Phys. 20, L124 (1981).

13. M.J. Helix, K.V. Vaidyanathan, B.G. Streetman, H.B. Dietrich, and P.K. Chatterjee, Thin Solid Films, 55, 143 (1978).

14. W.V. McLevige, P.K. Chatterjee, and B.G. Streetman, J. Phys. E: Sci. Instrum. 10, 335 (1977).

15. N. Holonyak, Jr. and D. Scifres, Rev. Sci. Instr. 42, 1885 (1971)

16. L.G. Van Uitert, P.K. Gallagher, S. Singh, and G.J. Zydzik, J. Vac. Sci. Technol. B, 1, 825 (1983).

17. J.D. Oberstar, B.G. Streetman, J.E. Baker, N.L. Finnegan, E.A. Samman, and Peter Williams, Thin Solid Films, 94, 149 (1982).

18. T. Onuma, T. Hirao, and T. Sugawa, J. Electrochem. Soc. 129, 837 (1982).

19. M.E. Greiner and J.F. Gibbons, Appl. Phys. Lett. 44, 750 (1984).

20. K.V. Vaidyanathan, M.J. Helix, D.J. Wolford, B.G. Streetman, R.J. Blattner, and C.A. Evans, Jr. J. Electrochem. Soc. 124, 1781 (1977).

21. M.E. Greiner and J.F. Gibbons, J. Appl. Phys. 57, 5181 (1985).

22. J.P. Donnelly, C.O. Bozler, and W.T. Lindley, Solid State Electronics, 20, 273 (1977).

23. C.W. Farley, T.S. Kim, T.R. Block, B.G. Streetman, and M. Anthony, in preparation.

2.6 Figure Titles

Figure 1. SIMS profiles of ^{30}Si and ^{31}P in unannealed Si_3N_4 deposited on InP at $350^\circ C$.

Figure 2. Low temperature ($4.2^\circ K$) PL spectra of unannealed InP encapsulated with PSG deposited at various temperatures.

Figure 3. SIMS profiles of ^{30}Si, ^{31}P, ^{54}Fe, and ^{113}In in annealed Si_3N_4 deposited on InP at $350^\circ C$.

Figure 4. SIMS profiles of ^{30}Si, ^{31}P, ^{54}Fe, and ^{113}In in annealed PSG deposited on InP at $300^\circ C$.

Figure 5. SIMS profiles of ^{30}Si in LEC and LPE SI InP encapsulated with different dielectrics. An implanted standard is shown for calibration of Si concentrations.

Figure 6. SIMS profiles of ^{54}Fe in LEC and LPE SI InP encapsulated with different dielectrics.
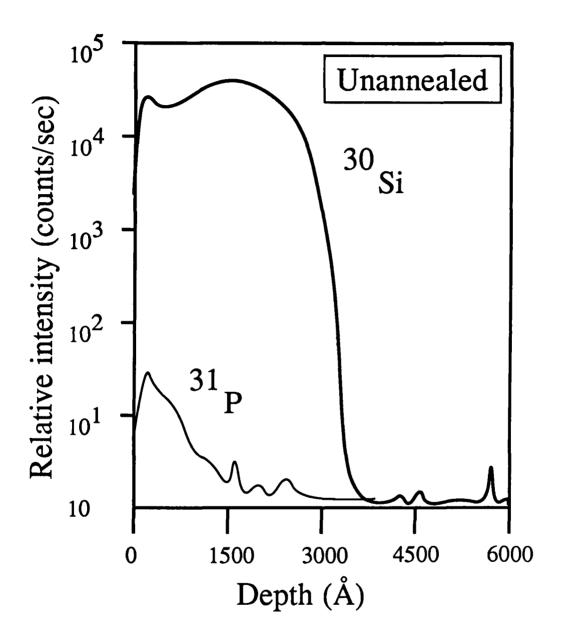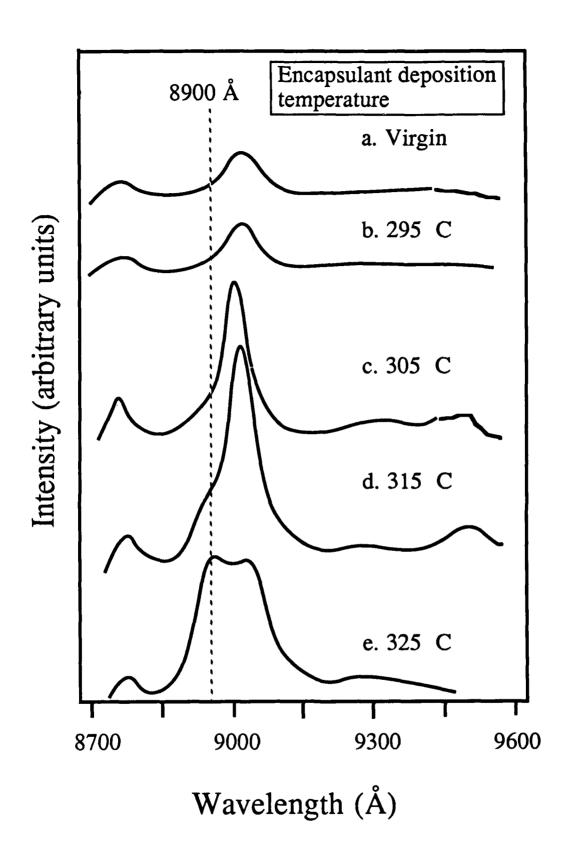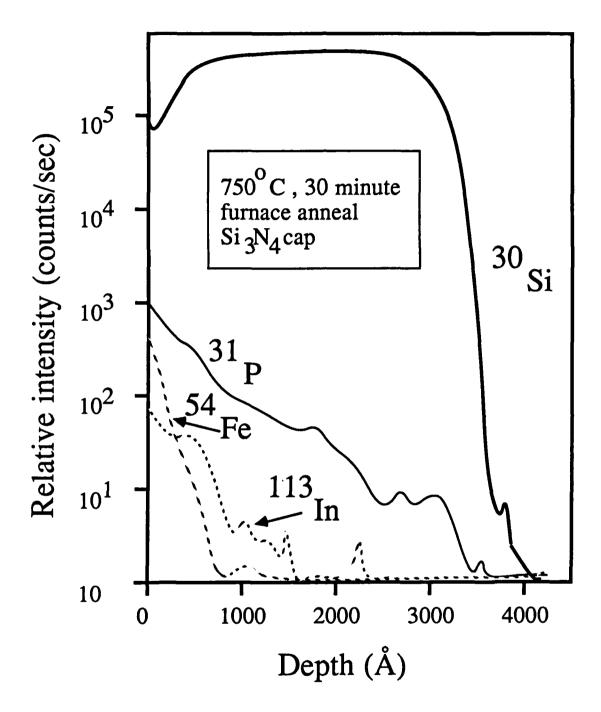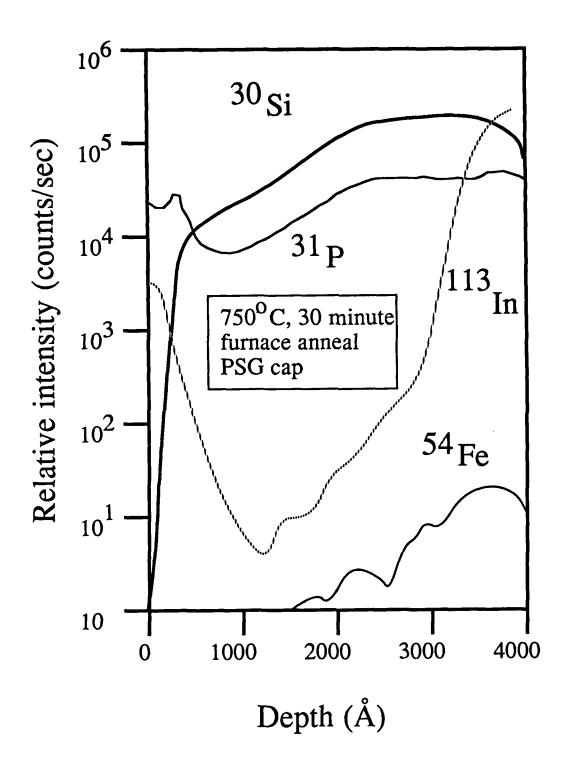
Figure 1.

Figure 2

38

The figure shows a SIMS depth profile plot with Relative intensity (counts/sec) on a logarithmic y-axis (10 to 10^5) versus Depth (Å) on the x-axis (0 to 4000). The inset text reads:

750°C, 30 minute furnace anneal Si_3N_4 cap

Curves are labeled ^{30}Si, ^{31}P, ^{54}Fe, and ^{113}In.

Figure 3

Figure 4

Figure 5

41

^{54}Fe
750°C , 30 minute
furnace anneal

Si$_3$N$_4$:LEC

PSG:LEC

Si$_3$N$_4$:LPE

Figure 6

42
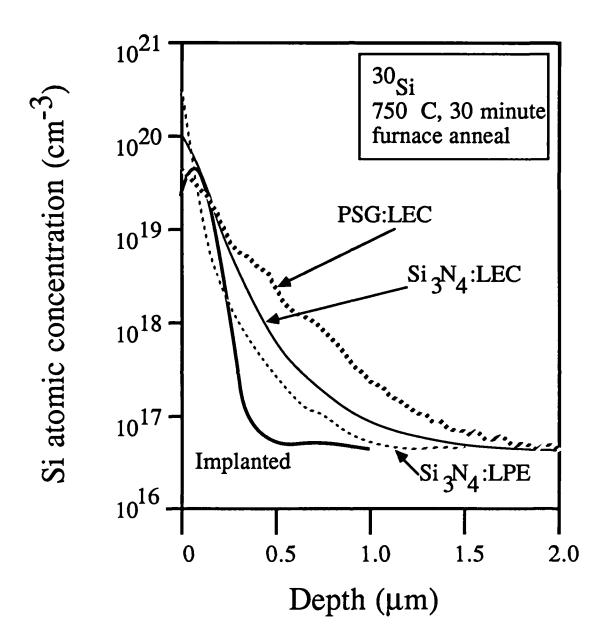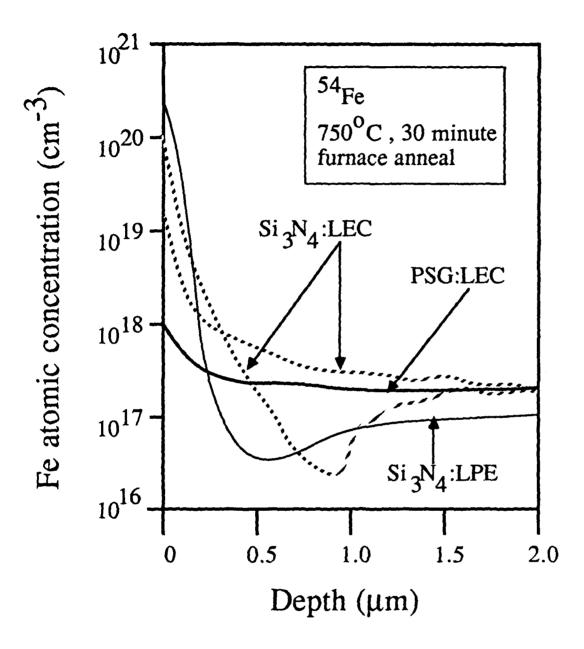
Chapter 3. Si Implantation Studies in InP

3.1 Furnace annealing

3.1.1 Co-implantation. Si activation during furnace annealing was studied for implant doses of 10^{14} to 10^{15} cm^{-2} at an energy of 150keV. First, appropriate anneal cycle times and temperatures were determined. Hall effect and PL measurements show that for a 30 minute anneal time, an anneal temperature of 750°C is necessary to produce complete annealing and activation. For an anneal temperature of 750°C, it is found that an anneal time of 20 to 30 minutes was necessary to achieve complete activation. 1 x 10^{14} cm^{-2}, 150keV Si + P and Si + Al co-implants were investigated in an attempt to reduce the autocompensation of Si donors by Si acceptors present in Si implanted InP. We investigated several variables in this co-implantation study including the energy of the P implant and the P dose and we observe decreased compensation for the co-implanted samples compared to those in which Si was implanted alone (Fig. 1). The post-anneal carrier concentration profile is found to depend heavily on the energy of the P co-implant. As can be seen in Figure 2, when the P implant energy is selected so that the projected range of the P is on the surface side of the projected range of the Si, higher carrier concentrations are observed near the surface then when Si is implanted alone. When the P is placed on the bulk side of the Si implant, activation was enhanced deeper in the bulk. This suggests that the P co-implant is influencing the site selection of Si and is causing a larger fraction of the Si to reside on In sites. We also investigated the effect of the dose of the co-implant and found that the maximum benefit could be achieved when the dose of the co-implant is approximately the same as the Si dose. As can be seen in Table 1, when the P dose is ten times less, the enhancement of activation is marginal. Although increasing the dose to ten times the P dose does increase the Si activation efficiency, the mobility is reduced so that no decrease in sheet resistance is observed.
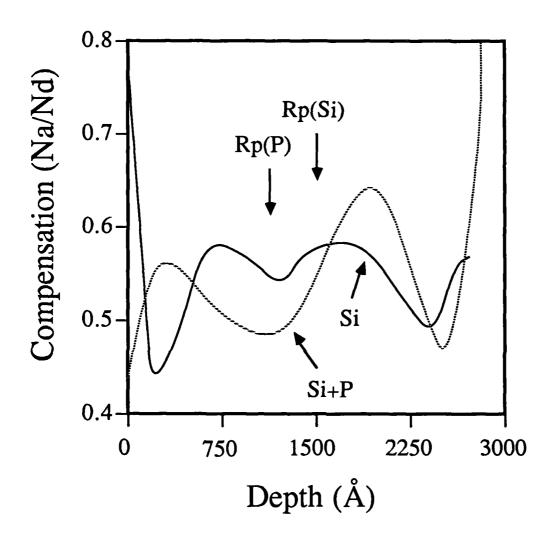
43

Figure 1. Compensation as a function of depth
for Si and Si+P implants into LEC InP:Fe show that
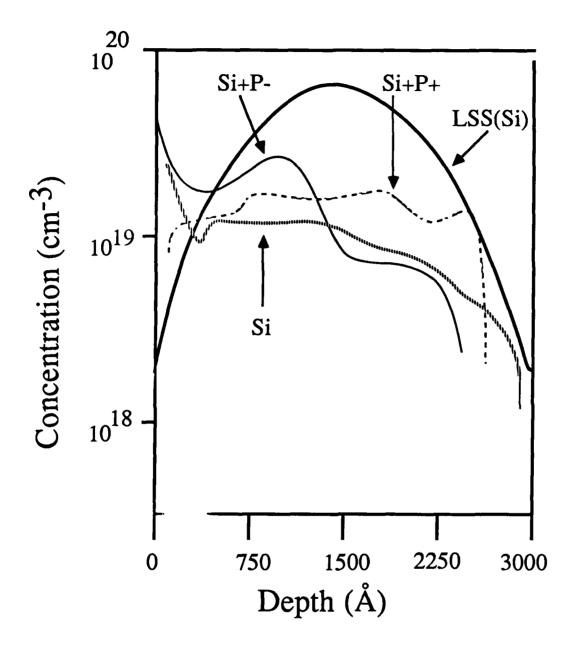the P co-implant reduces Si acceptor concentration

Figure 2. Hall profiles of Si and Si+P implants
show that activation is enhanced in the region where
the P co-implant is placed.

TABLE 1

Effect of P co-implant dose on a 150 keV, 1 x 10^{14} cm^{-2} Si implant activation

P dose (cm^{-2})	Sheet ρ (ohms/sq)	Mobility(cm^2/V.s)	Electron concentration (cm^{-2})
none	103	3230	1.87 x 10^{13}
1 x 10^{13}	170	1800	2.05 x 10^{13}
1 x 10^{14}	96	2025	3.19 x 10^{13}
1 x 10^{15}	193	1320	2.43 x 10^{13}

The lower mobility present in the samples with the highest P doses suggests that there may be incomplete annealing of implantation damage and possible formation of P precipitates. We also studies 10^{14} cm^{-2}, 150keV Si + N co-implants to see if the compensation of Si by N observed in GaAs occurs in InP. A surprising result was that the activation of Si + N was higher than when Si was implanted alone. This result is being investigated again to try to determine the nature of this effect.

3.1.2 Substrate Effects. The influence of compound stoichiometry on the activation behavior of Si implanted into InP has also been studied for both furnace and rapid thermal anneals. Si activation is higher in As-rich LEC substrates than in Ga-rich LPE substrates, which is expected since more Si should sit on As sites and act as an acceptor in the LPE material. In all cases, however, the carrier concentration saturates at a maximum value of about 1 x 10^{19} cm^{-3}, and there is evidence of very strong compensation of Si donors by Si acceptors.

3.2 Rapid Thermal Annealing

3.2.1 Isochronal anneals. The activation of Si implanted into InP using rapid thermal anneals has been studied. Isochronal anneals of 1 x 10^{15} cm^{-2}, 150keV implants have been performed and evidence of the effects of unequal recoil of In and P atoms during annealing has been seen. As can be seen in Figure 3, for all samples annealed between 550 and 750° C, there is a region on the surface side of the projected range which shows anomalously low carrier concentrations. This can be explained by the unequal recoil of In and P during annealing. P, which is much lighter than In, recoils much deeper during Si implantation and as a result, there is a
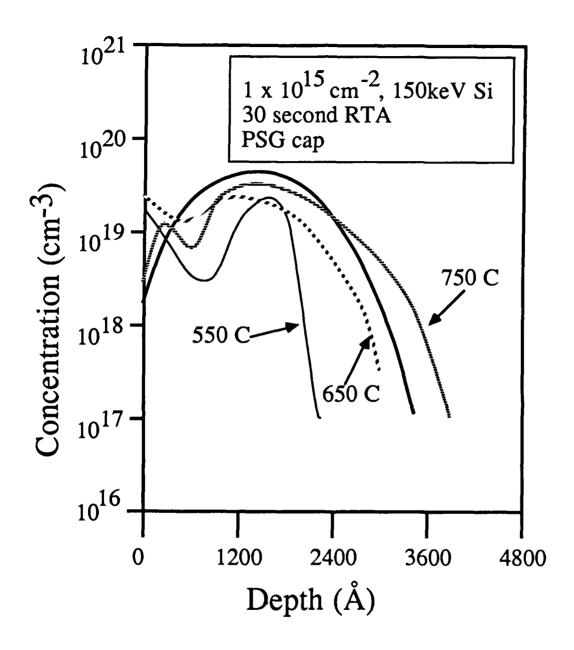
46

Figure 3. Hall profiles of Si implants activated with a 30 second RTA show the effects of unequal recoil.

net excess of In on the surface side of the projected range of the implant and a net excess of P on the bulk side of R_p. These fluctuations in stoichiometry influence the site selection of Si, causing more compensation on the surface side of R_p and less on the bulk side. As the anneal temperature increases, the carrier concentration profile extends further into the bulk, suggesting that even in 30 seconds the Si atoms may begin to diffues at 750°C. SIMS profiles of these samples are being taken to test this hypothesis.

3.2.2 Isothermal anneals. An investigation of the effects of the heating cycle in rapid thermal anneals was carried out. Experiments were done where the anneal time was varied from 0 seconds to 10 seconds, where a 0 second anneal corresponds to heating the sample to the anneal temperature and then immediately cooling it down. We found about 25% activation efficiency for the 0 second anneal and only an increase to 50% for a 10 second anneal . This result shows that a significant amount of annealing and activation occurs during the heating cycle as the temperature is raised from 300°C to the anneal temperature of 750°C, which takes about 5 seconds. Maximum activation efficiency is reached for high dose implants in about ten seconds, whereas lower dose implants can take up to 30 seconds. However, this time is much less than the three to five minutes needed to produce significant doping of the substrate from the encapsulant used during annealing.

3.2.3 Proximity cap annealing. We have also investigated the proximity cap annealing method for rapid thermal anneals. In this method, an InP wafer is placed in contact with another wafer (generally but not necessarily InP) which presumably prevents P from evaporating from the InP wafer during annealing. Several intersting results are observed. First, very little dependence on the type of wafer used as the proximity cap is found. We compared Si, GaAs, and InP and found that the activation efficiency of 1 x 10^{15} cm^{-2}, 150 keV implants was the same within experimental uncertainty for all three caps. This is more understandable when one considers the second unexpected result of these experiments. Profiles of the carrier concentration of these implants show a p-type layer on the surface which is about 500Å thick. This demonstrates that even for InP in close contact with another InP wafer, enough P can evaporate during annealing that Si atoms near the surface tend to occupy more P sites that In sites. This result suggests the use of controlled atmosphere annealing with an excess P overpressure provided by either PH_3 or solid P. Co-implants of Si + P and Si + Al were investigated for these high dose implants and it was found

48

that the effect of the P implants was less than in the encapsulated case and that Al co-implants had basically no effect on the Si activation efficiency. This is not surprising given the dramatic loss of P suspected during annealing, which would dominate the effect of any co-impalnts in determining the site selection behavior of Si.

    <u>3.2.4 Multistep annealing</u>. We also investigated the effect of a pre-anneal cycle to remove the structural damage before going to higher temperatures and attempting dopant activation. An enhancement of activation efficiency has been reported for pre-annealing of Si implants in GaAs. All anneals are carried out in a 10% H_2 in N_2 atmosphere. In these experiments, a sample is brought to an elevated temperature (100-600°C) for 30 seconds and then to the anneal temperature (in this case, 750°C) for the specified anneal time. In contrast to results seen in GaAs, no direct correlation is observed between pre-anneal temperature and electrical activation of 1×10^{15} cm^{-2}, 150 keV Si implants. Slightly lower sheet resistances are observed for 500°C pre-anneals, but we believe that the high implant doses may mask the effect of a pre-anneal cycle and this experiment might be more appropriate for lower Si implant doses.

3.3 Summary

Studies of the activation of Si using furnace and rapid thermal annealing and the effect of co-implantation on implant activation demonstrate several important points:

1. P co-implantation can be used to increase Si activation in both furnace and rapid thermal anneals.

2. The energy of the P co-implant is important because the activation of Si is enhanced in the region in which the P is implanted.

3. The dose of the P co-implant should be matched to the dose of the Si implant. Higher or lower doses produce higher sheet resistances.

4. Si activation is affected by the substrate stoichiometry; activation is greater in LEC material compared to LPE material.

5. Rapid thermal anneals of high dose Si implants produces carrier profiles with reduced activation near the surface which can be explained by unequal recoil of P atoms

during implantation. For short time anneals, P does not diffuse into the In-rich region so that reduced activation is seen in that region.

6. High dose Si implants appear to be activated very rapidly (<30 seconds), and significant annealing may occur during the heating of the sample up to the anneal temperature.

7. Investigations of proximity cap annealing show that for InP, the type of cap (SI, GaAs, InP) makes little difference in activation efficiency or sheet resistance.

8. Proximity cap annealed Si implants show a surface p-type layer which is presumably due to loss of P during annealing. This result suggests the use of controlled atmosphere annealing in a P overpressure to produce reliable activation in InP.

9. Investigation of the effect of a pre-anneal cycle on implant activation produced ambiguous results. No direct correlation could be observed between pre-anneal temperature and implant activation as has been reported in GaAs.

MISSION
of
Rome Air Development Center

RADC plans and executes research, development, test and selected acquisition programs in support of Command, Control, Communications and Intelligence (C³I) activities. Technical and engineering support within areas of competence is provided to ESD Program Offices (POs) and other ESD elements to perform effective acquisition of C³I systems. The areas of technical competence include communications, command and control, battle management, information processing, surveillance sensors, intelligence data collection and handling, solid state sciences, electromagnetics, and propagation, and electronic, maintainability, and compatibility.

END
1-87
DTIC